

Check for updates





ISSN 2053-2296

Received 12 March 2020 Accepted 7 May 2020

Edited by A. G. Oliver, University of Notre Dame, USA

CHEMISTRY

**Keywords:** halogen bonding; [2+2] cycloaddition reaction; organic solid state; crystal engineering; photoreactivity; cocrystal.

CCDC reference: 1947990

**Supporting information**: this article has supporting information at journals.iucr.org/c

## Crystal structure and photoreactivity of a halogenbonded cocrystal based upon 1,2-diiodoperchlorobenzene and 1,2-bis(pyridin-4-yl)ethylene

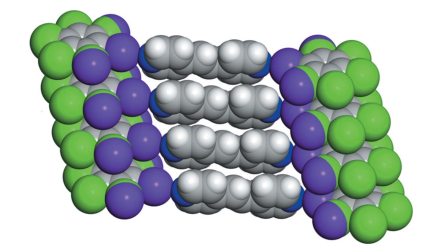
Eric Bosch, a Jessica D. Battleb and Ryan H. Groenemanb\*

<sup>a</sup>Department of Chemistry, Missouri State University, Springfield, Missouri 65897, USA, and <sup>b</sup>Department of Biological Sciences, Webster University, St Louis, Missouri 63119, USA. \*Correspondence e-mail: ryangroeneman19@webster.edu

The formation of a photoreactive cocrystal based upon 1,2-diiodoperchlorobenzene (1,2- $C_6I_2Cl_4$ ) and trans-1,2-bis(pyridin-4-yl)ethylene (BPE) has been achieved. The resulting cocrystal,  $2(1,2-C_6I_2Cl_4)\cdot(BPE)$  or  $C_6Cl_4I_2\cdot0.5C_{12}H_{10}N_2$ , comprises planar sheets of the components held together by the combination of  $I\cdots N$  halogen bonds and halogen–halogen contacts. Notably, the  $1,2-C_6I_2Cl_4$  molecules  $\pi$ -stack in a homogeneous and face-to-face orientation that results in an infinite column of the halogen-bond donor. As a consequence of this stacking arrangement and  $I\cdots N$  halogen bonds, molecules of BPE also stack in this type of pattern. In particular, neighbouring ethylene groups in BPE are found to be parallel and within the accepted distance for a photoreaction. Upon exposure to ultraviolet light, the cocrystal undergoes a solid-state [2+2] cycloaddition reaction that produces rctt-tetrakis(pyridin-4-yl)cyclobutane (TPCB) with an overall yield of 89%. A solvent-free approach utilizing dry vortex grinding of the components also resulted in a photoreactive material with a similar yield.

#### 1. Introduction

Halogen bonding continues to be a highly investigated noncovalent interaction applied to the formation of multicomponent materials in order to control their chemical properties (Priimagi et al., 2013). In particular, the photochemistry of halogen-bonded solids continues to be an active area of research in crystal engineering (Caronna et al., 2004). Recently, an increase in the number of halogen-bonded cocrystals that undergo a light-induced solid-state [2 + 2] cycloaddition reaction has been reported in the chemical literature (Sinnwell & MacGillivray, 2016; Sinnwell et al., 2018; Quentin et al., 2020). A continued focus in our research groups has been the utilization of halogen-bonding interactions to produce photoreactive cocrystals (Bosch et al., 2019a; Kruse et al., 2020). Specifically, we have reported the ability of 1,4diiodoperchlorobenzene (1,4-C<sub>6</sub>I<sub>2</sub>Cl<sub>4</sub>) to act as a halogenbonding template that organized *trans*-1,2-bis(pyridin-4-yl)ethylene (BPE) to undergo a cycloaddition reaction upon exposure to UV light (Bosch et al., 2019b). Key to the development of this photoreaction was the observation that **1,4-C<sub>6</sub>I<sub>2</sub>Cl<sub>4</sub>** prefers to  $\pi$ - $\pi$  stack in a face-to-face and homogeneous orientation, yielding an infinite column of the halogen-bond donor. As a consequence of this stacking arrangement and I···N halogen bonding, molecules of **BPE** also stack in an infinite array that positions the carbon-carbon double bond (C=C) in the correct orientation and separation distance to undergo a [2 + 2] cycloaddition reaction as stated by Schmidt's topochemical postulate (Schmidt, 1971).



© 2020 International Union of Crystallography

## research papers

Using this as inspiration, we report here the ability to form a photoreactive corrystal based upon 1,2-dijodoperchlorobenzene (1,2-C<sub>6</sub>I<sub>2</sub>Cl<sub>4</sub>) with BPE that undergoes a stereospecific photoreaction. As expected, the cocrystal 2(1,2- $C_6I_2CI_4)\cdot(BPE)$  is based upon  $I\cdot\cdot\cdot N$  halogen bonds and forms an extended solid. Similar to reported cocrystals containing 1,4-C<sub>6</sub>I<sub>2</sub>Cl<sub>4</sub>, molecules of 1,2-C<sub>6</sub>I<sub>2</sub>Cl<sub>4</sub> also  $\pi$ -stack in a face-toface and a homogeneous pattern to again form an infinite array. As before, molecules of BPE also form an infinite column that positions a pair of C=C groups in the correct orientation to undergo a solid-state photoreaction to form rctttetrakis(pyridin-4-yl)cyclobutane (TPCB) stereoselectively and in a high yield (see Scheme 1; a rendering of the components of the cocrystal, as well as the photoproduct from the solid-state [2 + 2] cycloaddition reaction). In addition to the solvent-based approach, we will also report the formation of a photoreactive solid that results from dry vortex grinding of both 1,2-C<sub>6</sub>I<sub>2</sub>Cl<sub>4</sub> and BPE with a similar yield for the photoreaction.

### 2. Experimental

### 2.1. Materials and general methods

The solvents toluene and ethanol, as well as the reactant molecule trans-1,2-bis(pyridin-4-yl)ethylene (**BPE**), were purchased from Sigma–Aldrich (St Louis, MO, USA) and were used as received. The halogen-bond donor 1,2-diiodoperchlorobenzene (**1,2-C<sub>6</sub>I<sub>2</sub>Cl<sub>4</sub>**) was synthesized according to a previously reported method (Reddy et al., 2006).

The [2+2] cycloaddition reactions were conducted in an ACE Glass photochemistry cabinet using UV radiation from a 450 W medium-pressure mercury lamp. The resulting cocrystal was placed between a pair of Pyrex glass plates for irradiation. The photoreactivity and the overall yield for the photoreaction were determined using  $^1H$  Nuclear Magnetic Resonance (NMR) spectroscopy on a Bruker Avance 400 MHz spectrometer using dimethyl sulfoxide (DMSO- $d_6$ ) as the solvent. Powder X-ray diffraction (PXRD) data for the cocrystal produced via dry vortex grinding were collected on a

Table 1
Experimental details.

Crystal data	
Chemical formula	$C_6Cl_4I_2 \cdot 0.5C_{12}H_{10}N_2$
$M_{ m r}$	558.77
Crystal system, space group	Triclinic, $P\overline{1}$
Temperature (K)	290
$a, b, c (\mathring{A})$	4.1177 (13), 13.502 (4), 14.151 (4)
$\alpha, \beta, \gamma \; (^\circ)$	78.864 (12), 83.719 (12), 87.935 (12)
$V(\mathring{A}^3)$	767.2 (4)
Z	2
Radiation type	Μο Κα
$\mu \text{ (mm}^{-1})$	4.78
Crystal size (mm)	$0.15 \times 0.08 \times 0.05$
Data collection	
Diffractometer	Bruker SMART APEX CCD area
2 minute meter	detector
Absorption correction	Multi-scan ( <i>SADABS</i> ; Bruker, 2016)
$T_{\min}$ , $T_{\max}$	0.783, 1.000
No. of measured, independent and observed $[I > 2\sigma(I)]$ reflections	11912, 3508, 2928
$R_{ m int}$	0.031
$(\sin \theta/\lambda)_{\max} (\mathring{A}^{-1})$	0.650
Refinement	
$R[F^2 > 2\sigma(F^2)], wR(F^2), S$	0.029, 0.065, 1.11
No. of reflections	3508
No. of parameters	191
No. of restraints	4
H-atom treatment	H-atom parameters constrained
$\Delta \rho_{\rm max}$ , $\Delta \rho_{\rm min}$ (e Å <sup>-3</sup> )	0.72, -0.59
computer programs: APEX2 (Bruker 2016)	SAINT (Bruker 2016) SHFLXT2018

computer programs: APEX2 (Bruker, 2016), SAINT (Bruker, 2016), SHELXT2018 (Sheldrick, 2015a), SHELXL2018 (Sheldrick, 2015b), SHELXTL (Bruker, 2016) and X-SEED (Barbour, 2001).

Rigaku Ultima IV X-ray diffractometer using Cu  $K\alpha_1$  radiation ( $\lambda = 1.54056 \text{ Å}$ ) between 5 and 40°  $2\theta$  at 290 K.

## 2.2. Synthesis and crystallization

The formation of the cocrystal  $2(\mathbf{1,2}\text{-}\mathbf{C_6I_2Cl_4}) \cdot (\mathbf{BPE})$  was achieved by dissolving  $\mathbf{1,2}\text{-}\mathbf{C_6I_2Cl_4}$  (50 mg) in toluene (3 ml), which was then combined with  $\mathbf{BPE}$  (10 mg) in ethanol (2 ml, 2:1 molar equivalents). Crystals suitable for X-ray diffraction formed within 2 d after some evaporation of the solvents.

#### 2.3. Refinement

Crystal data, data collection and structure refinement details are summarized in Table 1. During the refinement, the I atom halogen bonded to **BPE** refined smoothly, while the adjacent halogen atoms were clearly disordered, both exhibiting carbon-halogen distances intermediate between those expected for C-Cl and C-I. The relative populations of the disordered congeners were modeled with the help of a free variable and the respective C-Cl and C-I distances restrained to 1.7 (2) and 2.1 (2) Å, respectively. The free variable for this disorder refined to a final value of 0.59:0.41. The H atoms were treated using an appropriate riding model.

#### 3. Results and discussion

Crystallographic analysis revealed that  $2(1,2-C_6I_2Cl_4)\cdot(BPE)$  crystallizes in the centrosymmetric triclinic space group  $P\overline{1}$ .

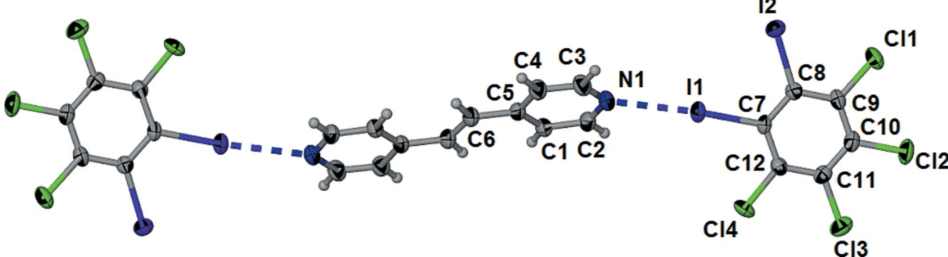


Figure 1

The labelled asymmetric unit of  $2(\mathbf{1,2-C_6I_2CI_4}) \cdot (\mathbf{BPE})$ , showing the extended halogen-bonded complex. The observed disorder has been omitted for clarity. Displacement ellipsoids are drawn at the 50% probability level for non-H atoms, while H atoms are shown as spheres of arbitrary size. Unlabeled atoms are related to their labeled congeners by (-x-1, -y, -z+2).

The asymmetric unit contains one molecule of 1,2- $C_6I_2Cl_4$  and half a molecule of **BPE**, where inversion symmetry generates the remainder of the molecule. The cocrystal is sustained by  $I \cdots N$  halogen bonds, with an  $I \cdots N$  distance of 2.871 (3) Å and a  $C-I \cdots N$  halogen-bond angle of 175.00 (11)°, as shown in Fig. 1.

The I atom forming the halogen bond is not disordered; however, the second I atom within 1,2-C<sub>6</sub>I<sub>2</sub>Cl<sub>4</sub> is disordered over both adjacent positions with a Cl atom as shown in Fig. 2. After refinement of the disorder, the occupancy factors for these disordered atoms converged to a final ratio of 0.59:0.41 at 290 K. The halobenzene rings form a planar network;

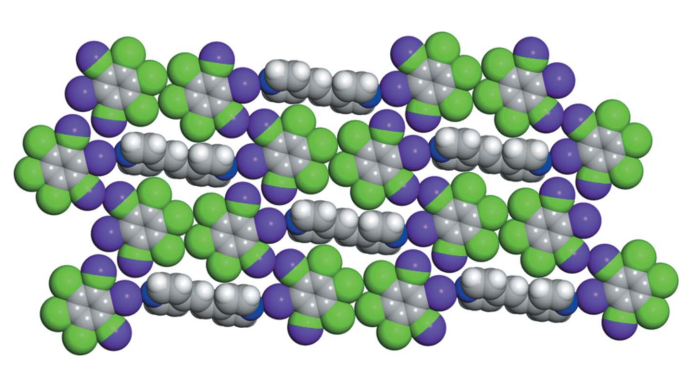


Figure 2 Partial view of the X-ray crystal structure of  $2(1,2\text{-}C_6I_2CI_4)\cdot(BPE)$ , illustrating the planar network of halobenzene molecules and the  $I\cdots N$  halogen bonding to various **BPE** molecules. The disordered I and Cl atoms are shown with split purple and green colors.

however, the **BPE** molecules are twisted with respect to the plane defined by the halobenzenes, as shown in Fig. 1. The dihedral angle between the planes of **1,2-C<sub>6</sub>I<sub>2</sub>Cl<sub>4</sub>** and the pyridine ring of **BPE** was 53.77 (9)°.

The two-dimensional arrangement of the halobenzenes is supported by two crystallographically unique  $I \cdots I$  contacts, which are shown in detail as X and Y in Fig. 3. These  $I \cdots I$  contacts include both Type I and Type II halogen–halogen interactions (Desiraju & Parthasarathy, 1989; Mukherjee *et al.*, 2014).

The Type I halogen-halogen interaction between disordered I atoms (**X**) has an  $I2A \cdots I2A^i$  distance of 3.296 (5) Å [symmetry code: (i) -x + 1, -y, -z + 1], with bond angles of  $\theta 1 = \theta 2 = 143.2$  (2)°. The alternate halogen-halogen interaction, corresponding to the second position of the disordered I atom (**Y**), also features a Type I halogen-halogen contact supported by a Type II halogen-halogen interaction. This Type I halogen-halogen distance,  $I2 \cdots I2^{ii}$ , is 3.736 (4) Å [symmetry code: (ii) -x, -y + 1, -z + 1], with bond angles of  $\theta 1 = \theta 2 = 123.67$  (14)°. The weaker Type II I  $\cdots$  I contact has an  $I1 \cdots I2^{ii}$  distance of 3.885 (2) Å, with bond angles of  $\theta 1 = 178.78$  (12)° and  $\theta 2 = 118.30$  (10)°.

The three-dimensional structure of the cocrystal is dominated by homogeneous infinite face-to-face offset  $\pi-\pi$  stacking of the halogen-bond donor **1,2-C<sub>6</sub>I<sub>2</sub>Cl<sub>4</sub>**, similar to what was observed previously in the cocrystal (**1,4-C<sub>6</sub>I<sub>2</sub>Cl<sub>4</sub>**)·(**BPE**) (Bosch *et al.*, 2019*b*). The **1,2-C<sub>6</sub>I<sub>2</sub>Cl<sub>4</sub>** centroid-to-centroid distance is 4.1177 (13) Å, corresponding to the

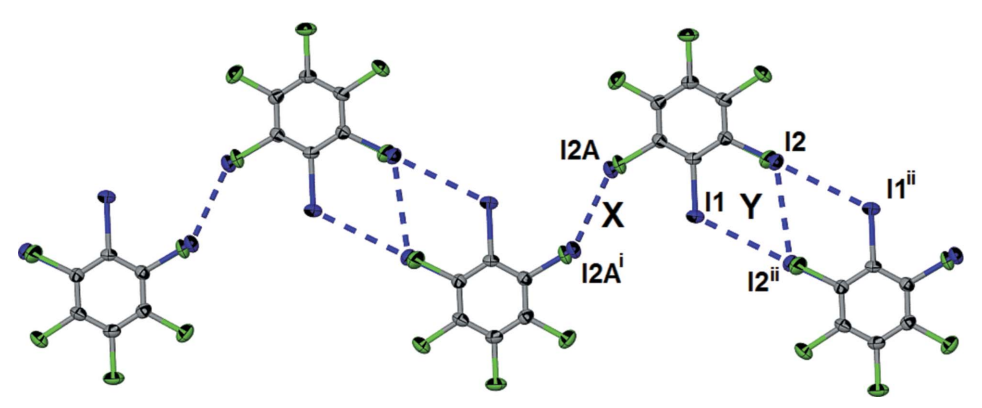
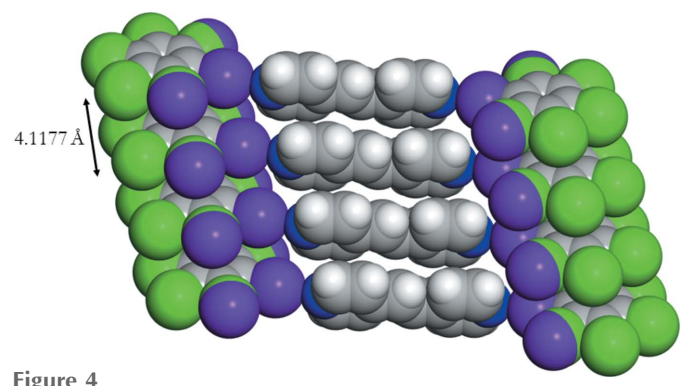


Figure 3
Partial view of the side-by-side packing of five 1,2-C<sub>6</sub>I<sub>2</sub>Cl<sub>4</sub> molecules highlighting the Type I halogen–halogen interaction (**X**) and the second Type I and Type II interactions (**Y**). The disordered I and Cl atoms are shown with split purple and green colors. Symmetry codes are defined in the text.

crystallographic a axis, and due to crystal symmetry, the distance between neighboring pairs of C=C groups. As a result, the separation distance of the C=C groups is within the accepted limit of 4.2 Å for a solid-state [2+2] cycloaddition reaction (Schmidt, 1971). Lastly, since nearest C=C groups within neighboring **BPE** are also found to be parallel and coplanar, this meets all of the requirements for a photoreaction as shown in Fig. 4.

To determine if a [2+2] cycloaddition reaction would occur, a powdered sample of 2(1,2-C<sub>6</sub>I<sub>2</sub>Cl<sub>4</sub>)·(BPE) was dried, placed between glass plates, and put in a photoreactor cabinet where it was subjected to broadband UV radiation. A photoreaction was confirmed, as evidenced by the decrease of the olefinic peak for BPE at 7.58 ppm (Fig. S1 in the supporting information), along with the concomitant appearance of the cyclobutane peak at 4.70 ppm (Fig. S2 in the supporting information) in the <sup>1</sup>H NMR spectrum that confirms the formation of the photoproduct TPCB (MacGillivray et al., 2000). An overall yield of 89% for the photoreaction was determined by <sup>1</sup>H NMR spectroscopy after 60 h of irradiation (Fig. S2 in the supporting information) and no further reaction was observed after additional irradiation. It is noteworthy that the solid-state photoreaction of the cocrystal formed between 1,4-C<sub>6</sub>I<sub>2</sub>Cl<sub>4</sub> and BPE also had a yield of 89% (Bosch et al., 2019b). The structural reason behind the incomplete photoreaction is unclear.

As an alternative to a solvent-based approach, we also explored cocrystallization *via* solvent-free dry vortex grinding. Thus, a sample comprised of 100 mg of **1,2-C<sub>6</sub>I<sub>2</sub>Cl<sub>4</sub>** and 20 mg of **BPE** (2:1 molar equivalents) was added to a 15 ml SmartSnap Grinding Jar with two steel BBs (5 mm diameter) and was ground using a VWR Vortex Genie 2 for a total of 15 min. At the 5 and 10 min marks, the resulting solid was scraped from the edges and then the grinding was resumed. To study the bulk properties of the resulting solid, the vortexed sample was studied *via* powder X-ray diffraction. The observed diffractogram indicates a different phase formed *via* dry vortex grinding when compared to the calculated powder pattern for 2(**1,2-C<sub>6</sub>I<sub>2</sub>Cl<sub>4</sub>**)·(**BPE**) (Fig. S4 in the supporting information).



Partial view of the X-ray crystal structure of  $2(\mathbf{1},\mathbf{2}-\mathbf{C}_6\mathbf{I}_2\mathbf{Cl}_4)\cdot(\mathbf{BPE})$ , illustrating the homogenous infinite face-to-face offset  $\pi-\pi$  stacking of the aromatic rings. The disordered I and Cl atoms are shown with split purple and green colors.

The material resulting from dry vortex grinding was placed in the photoreactor cabinet and exposed to UV radiation as before. <sup>1</sup>H NMR spectroscopy again confirmed the formation of the photoproduct **TPCB** by both the partial loss of the olefinic peak for **BPE** at 7.58 ppm and the appearance of a cyclobutane peak at 4.70 ppm (MacGillivray *et al.*, 2000). The overall yield for the photoreaction was again determined to be 89% after 60 h of UV exposure (Fig. S3 in the supporting information). Thus, both the solvent-based and solvent-free approaches had a similar yield for the photoreaction even though they had different powder patterns. It should also be noted that a similar yield for the photoreaction (*i.e.* 89%) was observed for the cocrystal based upon **1,4-C<sub>6</sub>I<sub>2</sub>Cl<sub>4</sub>** and **BPE** using a solvent-free approach (Bosch *et al.*, 2019b).

#### 4. Conclusion

In this article, we have described the synthesis, crystal structure, and photoreactivity of the cocrystal  $2(\mathbf{1,2\text{-}C_6I_2CI_4})\cdot(\mathbf{BPE})$  that is held together by the combination of  $I\cdots N$  halogen bonds, halogen-halogen contacts, and  $\pi-\pi$  stacking interactions. Indeed, the homogeneous and face-to-face  $\pi-\pi$  stacking of  $\mathbf{1,2\text{-}C_6I_2CI_4}$  molecules along with the  $I\cdots N$  halogen bonds position a pair of C=C groups within  $\mathbf{BPE}$  in a suitable position to undergo a [2+2] cycloaddition reaction. A similar photoreactive solid was also achieved *via* dry vortex grinding. Currently, we are investigating the ability of  $\mathbf{1,2\text{-}C_6I_2CI_4}$  to template additional photoreactions with other olefin-containing compounds.

### Acknowledgements

RHG gratefully acknowledges financial support from Webster University in the form of various Faculty Research Grants.

## **Funding information**

Funding for this research was provided by: National Science Foundation (grant No. MRI, CHE-1827756).

## References

Barbour, L. J. (2001). J. Supramol. Chem. 1, 189–191.

Bosch, E., Kruse, S. J., Krueger, H. R. Jr & Groeneman, R. H. (2019b). *Cryst. Growth Des.* **19**, 3092–3096.

Bosch, E., Kruse, S. J., Reinheimer, E. W., Rath, N. P. & Groeneman, R. H. (2019a). CrystEngComm, 21, 6671–6675.

Bruker (2016). APEX2, SAINT, SHELXTL, and SADABS. Bruker AXS Inc., Madison, Wisconsin, USA.

Caronna, T., Liantonio, R., Logothetis, T. A., Metrangolo, P., Pilati, T. & Resnati, G. (2004). *J. Am. Chem. Soc.* **126**, 4500–4501.

Desiraju, G. R. & Parthasarathy, R. (1989). J. Am. Chem. Soc. 111, 8725–8726.

Kruse, S. J., Bosch, E., Brown, F. & Groeneman, R. H. (2020). *Cryst. Growth Des.* **20**, 1969–1974.

MacGillivray, L. R., Reid, J. L. & Ripmeester, J. A. (2000). J. Am. Chem. Soc. 122, 7817–7818.

Mukherjee, A., Tothadi, S. & Desiraju, G. R. (2014). *Acc. Chem. Res.* **47**, 2514–2524.

Priimagi, A., Cavallo, G., Metrangolo, P. & Resnati, G. (2013). Acc. Chem. Res. 46, 2686–2695.

- Quentin, J., Swenson, D. C. & MacGillivray, L. R. (2020). *Molecules*, **25**, 907–919.
- Reddy, C. M., Kirchner, M. T., Gundakaram, R. C., Padmanabhan, K. A. & Desiraju, G. R. (2006). *Chem. Eur. J.* **12**, 2222–2234.
- Schmidt, G. J. M. (1971). J. Pure Appl. Chem. 27, 647-678.
- Sheldrick, G. M. (2015a). Acta Cryst. A71, 3-8.
- Sheldrick, G. M. (2015b). Acta Cryst. C71, 3-8.
- Sinnwell, M. A., Blad, J. N., Thomas, L. R. & MacGillivray, L. R. (2018). *IUCrJ*, **5**, 491–496.
- Sinnwell, M. A. & MacGillivray, L. R. (2016). *Angew. Chem. Int. Ed.* **55**, 3477–3480.

 $2\sigma(I)$ 

## supporting information

Acta Cryst. (2020). C76, 557-561 [https://doi.org/10.1107/S2053229620006233]

Crystal structure and photoreactivity of a halogen-bonded cocrystal based upon 1,2-diiodoperchlorobenzene and 1,2-bis(pyridin-4-yl)ethylene

## Eric Bosch, Jessica D. Battle and Ryan H. Groeneman

## **Computing details**

Data collection: APEX2 (Bruker, 2016); cell refinement: SAINT (Bruker, 2016); data reduction: SAINT (Bruker, 2016); program(s) used to solve structure: SHELXT2018 (Sheldrick, 2015a); program(s) used to refine structure: SHELXL2018 (Sheldrick, 2015b); molecular graphics: SHELXTL (Bruker, 2016) and X-SEED (Barbour, 2001); software used to prepare material for publication: SHELXTL (Bruker, 2016).

1,2-Diiodo-3,4,5,6-chlorobenzene–*trans*-1,2-bis(pyridin-4-yl)ethylene (2/1)

## Crystal data

$C_6Cl_4I_2 \cdot 0.5C_{12}H_{10}N_2$	Z = 2
$M_r = 558.77$	F(000) = 516
Triclinic, $P\overline{1}$	$D_{\rm x} = 2.419 {\rm Mg m}^{-3}$
a = 4.1177 (13)  Å	Mo $K\alpha$ radiation, $\lambda = 0.71073 \text{ Å}$
b = 13.502 (4)  Å	Cell parameters from 5904 reflections
c = 14.151 (4)  Å	$\theta = 2.3-27.5^{\circ}$
$\alpha = 78.864 (12)^{\circ}$	$\mu = 4.78 \text{ mm}^{-1}$
$\beta = 83.719 (12)^{\circ}$	T = 290  K
$\gamma = 87.935 (12)^{\circ}$	Rod, yellow
$V = 767.2 (4) \text{ Å}^3$	$0.15 \times 0.08 \times 0.05 \text{ mm}$

## Data collection

Bruker SMART APEX CCD area detector	11912 measured reflections
diffractometer	3508 independent reflections
Radiation source: sealed tube	2928 reflections with $I > 2\sigma(I)$
Detector resolution: 8 pixels mm <sup>-1</sup>	$R_{\rm int} = 0.031$
$\omega$ and $\varphi$ scans	$\theta_{\text{max}} = 27.5^{\circ}, \ \theta_{\text{min}} = 2.3^{\circ}$
Absorption correction: multi-scan	$h = -5 \longrightarrow 5$
(SADABS; Bruker, 2016)	$k = -17 \longrightarrow 17$
$T_{\min} = 0.783, T_{\max} = 1.000$	$l = -18 \longrightarrow 18$

### Refinement

Kejinemeni	
Refinement on $F^2$	Hydrogen site location: inferred from
Least-squares matrix: full	neighbouring sites
$R[F^2 > 2\sigma(F^2)] = 0.029$	H-atom parameters constrained
$wR(F^2) = 0.065$	$w = 1/[\sigma^2(F_0^2) + (0.0213P)^2 + 0.601P]$
S = 1.11	where $P = (F_0^2 + 2F_c^2)/3$
3508 reflections	$(\Delta/\sigma)_{\rm max} = 0.002$
191 parameters	$\Delta \rho_{\mathrm{max}} = 0.72  \mathrm{e  \mathring{A}^{-3}}$
4 restraints	$\Delta  ho_{\mathrm{min}} = -0.58 \; \mathrm{e} \; \mathrm{\AA}^{-3}$

## Special details

**Geometry**. All esds (except the esd in the dihedral angle between two l.s. planes) are estimated using the full covariance matrix. The cell esds are taken into account individually in the estimation of esds in distances, angles and torsion angles; correlations between esds in cell parameters are only used when they are defined by crystal symmetry. An approximate (isotropic) treatment of cell esds is used for estimating esds involving l.s. planes.

**Refinement.** A single crystal of  $2(1,2-C_6I_2Cl_4)$ .(BPE) was mounted on a MiTeGen cryoloop in a random orientation for X-ray data collection. A Bruker Venture Duo Photon-II single-crystal X-ray diffractometer equipped with an Oxford Cryostream device was used for the data collection. APEXII and SAINT software packages (Bruker, 2016) were used for data collection and integration, respectively. The data were corrected for systematic errors using SADABS based on the Laue symmetry using equivalent reflections. The structure was solved by dual space methods using SHELXT-2018 (Sheldrick, 2015a) and refined against  $F^2$  using SHELXL-2018 (Sheldrick, 2015b). The program X-Seed was used as a graphical interface (Barbour, 2001).

Fractional atomic coordinates and isotropic or equivalent isotropic displacement parameters  $(\mathring{A}^2)$ 

	x	y	Z	$U_{ m iso}$ */ $U_{ m eq}$	Occ. (<1)
I1	0.24195 (6)	0.26852(2)	0.51627(2)	0.04165 (9)	
Cl1	0.5409(3)	0.54003 (8)	0.15189 (8)	0.0619(3)	
C12	0.9278 (3)	0.37431 (9)	0.06306 (7)	0.0645 (3)	
I2	0.2089 (4)	0.51541 (16)	0.37413 (14)	0.0477 (2)	0.5895 (13)
C13	0.9897(3)	0.15892 (8)	0.18345 (8)	0.0581 (3)	
Cl4	0.658(2)	0.1062 (4)	0.3924 (6)	0.0592 (14)	0.5895 (13)
N1	-0.0686 (8)	0.2054(2)	0.7094(2)	0.0477 (8)	
C7	0.4609 (8)	0.3024(2)	0.3720(2)	0.0333 (7)	
C8	0.4379 (8)	0.3997(2)	0.3175 (2)	0.0347 (7)	
C12	0.6292(8)	0.2279(2)	0.3300(2)	0.0358 (7)	
C11	0.7737 (8)	0.2506(3)	0.2351(3)	0.0385 (8)	
C9	0.5790 (9)	0.4211 (3)	0.2214(3)	0.0403 (8)	
C10	0.7492 (9)	0.3466 (3)	0.1810(3)	0.0416 (8)	
C2	-0.2387 (9)	0.1216(3)	0.7194(3)	0.0457 (9)	
H2	-0.275618	0.098770	0.663601	0.055*	
C1	-0.3637 (9)	0.0665(3)	0.8074(3)	0.0415 (8)	
H1	-0.484620	0.008961	0.810271	0.050*	
C4	-0.1303 (10)	0.1856 (3)	0.8812(3)	0.0484 (9)	
H4	-0.087602	0.210442	0.935376	0.058*	
C5	-0.3065(9)	0.0981(3)	0.8920(3)	0.0400(8)	
C3	-0.0176 (10)	0.2361 (3)	0.7893(3)	0.0510 (10)	
Н3	0.100320	0.294730	0.783742	0.061*	
C6	-0.4232 (9)	0.0435 (3)	0.9892(3)	0.0450 (9)	
Н6	-0.384953	0.073143	1.040995	0.054*	
Cl4A	0.244(3)	0.4982 (9)	0.3684 (9)	0.075(3)	0.4105 (13)
I2A	0.6649 (7)	0.08069 (16)	0.4059(2)	0.0485 (4)	0.4105 (13)

## Atomic displacement parameters $(\mathring{A}^2)$

	$U^{11}$	$U^{22}$	$U^{33}$	$U^{12}$	$U^{13}$	$U^{23}$
I1	0.04061 (14)	0.05105 (15)	0.03022 (13)	-0.00472 (10)	0.00041 (9)	-0.00170 (10)
Cl1	0.0889(8)	0.0433 (5)	0.0455 (6)	-0.0013(5)	-0.0026(5)	0.0088 (4)
Cl2	0.0877 (8)	0.0682 (7)	0.0331 (5)	-0.0121 (6)	0.0149 (5)	-0.0081 (5)

Acta Cryst. (2020). C**76**, 557-561 sup-2

# supporting information

I2	0.0535 (5)	0.0474 (5)	0.0425 (4)	0.0125 (5)	-0.0025 (4)	-0.0128(3)
C13	0.0621 (6)	0.0582 (6)	0.0582 (6)	0.0053 (5)	0.0033 (5)	-0.0277(5)
Cl4	0.0847 (19)	0.029(2)	0.057(2)	0.0114 (19)	-0.0050(15)	0.0052 (17)
N1	0.0558 (19)	0.0425 (17)	0.0384 (18)	-0.0010 (14)	0.0027 (15)	0.0038 (14)
C7	0.0318 (16)	0.0427 (18)	0.0249 (16)	-0.0064 (13)	-0.0022(13)	-0.0046 (13)
C8	0.0361 (17)	0.0366 (17)	0.0329 (18)	-0.0028 (13)	-0.0070(14)	-0.0082 (14)
C12	0.0363 (17)	0.0356 (17)	0.0349 (18)	-0.0038 (13)	-0.0067 (14)	-0.0033 (14)
C11	0.0363 (18)	0.0428 (19)	0.039(2)	-0.0047 (14)	-0.0026 (15)	-0.0153 (15)
C9	0.047(2)	0.0399 (19)	0.0316 (18)	-0.0083 (15)	-0.0061 (16)	0.0005 (14)
C10	0.044(2)	0.049(2)	0.0317 (19)	-0.0094 (16)	0.0006 (16)	-0.0082 (16)
C2	0.059(2)	0.050(2)	0.0276 (18)	0.0062 (18)	-0.0047(17)	-0.0057 (15)
C1	0.048(2)	0.0381 (18)	0.036(2)	-0.0018 (15)	-0.0018 (16)	-0.0031 (15)
C4	0.065(2)	0.045 (2)	0.036(2)	-0.0046 (18)	-0.0043 (18)	-0.0091 (16)
C5	0.0452 (19)	0.0411 (19)	0.0314 (18)	0.0047 (15)	-0.0022 (15)	-0.0034 (15)
C3	0.062(3)	0.041(2)	0.047(2)	-0.0095 (18)	-0.002(2)	-0.0026(17)
C6	0.056(2)	0.046(2)	0.0309 (19)	0.0017 (16)	-0.0017 (17)	-0.0039 (16)
Cl4A	0.083 (4)	0.070 (5)	0.061 (4)	0.035(3)	0.015(2)	-0.007(3)
I2A	0.0628 (6)	0.0329 (10)	0.0472 (8)	0.0021 (7)	-0.0074 (5)	-0.0007(7)

## Geometric parameters (Å, °)

Geometric parameters (A,	/		
I1—C7	2.110 (3)	C11—C10	1.378 (5)
C11—C9	1.726 (4)	C9—C10	1.384 (5)
C12—C10	1.725 (4)	C2—C1	1.379 (5)
I2—C8	2.046 (4)	C2—H2	0.9300
C13—C11	1.728 (4)	C1—C5	1.391 (5)
C14—C12	1.716 (6)	C1—H1	0.9300
N1—C3	1.316 (5)	C4—C5	1.383 (5)
N1—C2	1.328 (5)	C4—C3	1.385 (5)
C7—C12	1.392 (5)	C4—H4	0.9300
C7—C8	1.395 (5)	C5—C6	1.469 (5)
C8—C9	1.398 (5)	С3—Н3	0.9300
C8—Cl4A	1.758 (11)	C6—C6 <sup>i</sup>	1.320 (7)
C12—C11	1.390 (5)	C6—H6	0.9300
C12—I2A	2.077 (4)		
C3—N1—C2	117.0 (3)	C11—C10—C12	120.5 (3)
C12—C7—C8	119.1 (3)	C9—C10—Cl2	119.8 (3)
C12—C7—I1	120.5 (2)	N1—C2—C1	123.9 (4)
C8—C7—I1	120.4 (2)	N1—C2—H2	118.0
C7—C8—C9	120.0(3)	C1—C2—H2	118.0
C7—C8—C14A	121.1 (5)	C2—C1—C5	119.1 (3)
C9—C8—C14A	118.8 (5)	C2—C1—H1	120.4
C7—C8—I2	122.1 (3)	C5—C1—H1	120.4
C9—C8—I2	117.9 (3)	C5—C4—C3	119.7 (4)
C11—C12—C7	120.2 (3)	C5—C4—H4	120.1
C11—C12—C14	118.4 (4)	C3—C4—H4	120.1
C7—C12—C14	121.3 (4)	C4—C5—C1	116.7 (3)

Acta Cryst. (2020). C**76**, 557-561 sup-3

# supporting information

C11—C12—I2A	118.5 (3)	C4—C5—C6	120.1 (3)	
C7—C12—I2A	121.2 (3)	C1—C5—C6	123.3 (3)	
C10—C11—C12	120.6 (3)	N1—C3—C4	123.5 (4)	
C10—C11—Cl3	119.0 (3)	N1—C3—H3	118.3	
C12—C11—Cl3	120.3 (3)	C4—C3—H3	118.3	
C10—C9—C8	120.2 (3)	C6 <sup>i</sup> —C6—C5	126.7 (5)	
C10—C9—C11	119.3 (3)	C6 <sup>i</sup> —C6—H6	116.6	
C8—C9—C11	120.5 (3)	C5—C6—H6	116.6	
C11—C10—C9	119.7 (3)			

Symmetry code: (i) -x-1, -y, -z+2.

## Hydrogen-bond geometry (Å, °)

D— $H$ ··· $A$	<i>D</i> —H	$H\cdots A$	D··· $A$	<i>D</i> —H··· <i>A</i>
C2—H2···I2A <sup>ii</sup>	0.93	3.31	4.072 (5)	141

Symmetry code: (ii) -x, -y, -z+1.